

**EVALUATION OF ASCE/SEI 7 DIRECTION OF
LOADING PROVISIONS USING CSMIP RECORDS**

Reid B. Zimmerman, P.E.
Bret Lizundia, S.E.
Saeed Fathali, Ph.D., P.E.

Rutherford + Chekene
Structural and Geotechnical Engineers
San Francisco, CA

Abstract

The data recorded from seismically instrumented buildings over the past approximately 40 years is used to indirectly evaluate the ASCE/SEI 7 direction of loading provisions. Direction of loading provisions require combining the maximum response in one direction, with a percentage of the maximum response in the orthogonal direction. In ASCE/SEI 7, a value of 30% is used for response in the orthogonal direction. This research shows that, for a wide range of conditions and assumptions, building response exceeds combinations with maximum response in one direction and only 30% of the maximum in the other direction. Alternative combination values are provided that better bound the recorded data.

Research Motivation and Limitations

The foundation of the direction of loading provisions in ASCE/SEI 7-10 (ASCE, 2010) date back to Newmark (1975) and Rosenblueth and Contreras (1977) and have remained relatively unchanged as codes have evolved in other ways. Direction of loading provisions often use the shorthand of 100%+XX% where XX% is the percentage of the maximum in the orthogonal direction. Past research on orthogonal combination criteria has almost universally concluded that a 100%+30% criterion is unconservative, although the literature differs on the degree of unconservatism. For a complete literature review and extensive background, refer to Zimmerman et al. (2014). Most of the research on direction of loading provisions since Rosenblueth and Contreras (1977) proposed the 100%+30% criterion has focused on analytical studies based on computer simulations of building or bridge response (e.g., MacRae and Mattheis, 2000; Zaghlool et al., 2001; MacRae and Tagawa, 2001; Sherman and Okazaki, 2010; Bisadi and Head, 2011; Cimellaro et al., 2014) or on theoretical studies based on generalized parameters (e.g., Menun and Der Kiureghian, 1998; Hernandez and Lopez, 2002; Lopez et al., 2001).

No studies, however, have attempted to use actual earthquake data from instrumented buildings as pursued in this research. The Center for Engineering Strong Motion Data (CESMD, 2015) provides an extensive set of instrumented building records that are used in this research. Using actual building response records, though, has limitations which include the following:

1. The component responses (e.g., moments, shears, etc.) are not available. For example, axial load in a column shared by two intersecting lateral force-resisting systems is not recorded as part of building instrumentation.
2. As compared to analytical studies, it is not possible to design a building to a specific provision and then assess its adequacy. Instead, only the response from an earthquake (which is not necessarily equivalent to a design-basis earthquake) is available while information about building capacity is missing. For example, with only the building response available, a building cannot be designed per the ASCE/SEI 7 (ASCE, 2010) direction of loading provisions and then assessed against the permissible probability of collapse (i.e., the FEMA P695 procedure) (FEMA, 2009).

The first limitation is less restrictive than the second since even an evaluation of a limited set of response types is valuable. The second limitation is more restrictive because assessment of an ASCE/SEI 7 (ASCE, 2010) provision is inherently a comparison of demand (i.e., response) versus capacity. While the demand, available through the recorded building response, is more directly obtained in this research than in analytical studies, the capacity is essentially unavailable. However, it should be noted that the building capacity is not used in the ASCE/SEI 7 direction of loading provisions. Instead, 100% and 30% of the respective demands are. It is, therefore, possible to make an assessment of the *application* of the provisions (i.e., combining 100% and 30% of the demand) even if an assessment of the *effect* of the provisions (i.e., the collapse probability of the resulting design) cannot be made. In other words, this research cannot answer the question: "Does a building designed to the ASCE/SEI 7-10 direction of loading provisions including a 100%+30% criterion have a sufficiently low probability of collapse to meet the intent of provisions?" But this research can answer: "Does an approximation of the actual response, using a 100%+30% criterion, adequately bound the actual response of a building during a real earthquake?"

Presumed Intent of the Direction of Loading Provisions

Before asking how to evaluate a 100%+30% criterion using instrumented building data, it is important to ask what the intent of the 100%+30% criterion is in ASCE/SEI 7-10 (ASCE, 2010). The commentary of ASCE/SEI 7-10 for the direction of loading provisions lacks specificity. While it does directly reference Rosenblueth and Contreras (1977), it does not describe the type of earthquake phenomenon the provisions intend to bound. Instead, engineers and researchers are left to infer the intention of the provisions when facing the following questions:

- Is the intent to account for correlation between the two directions of ground motion? In other words, is the intent to account for the fact that earthquake demand at 45 degrees with respect to the building axes could be as large as the earthquake demand along the x- or y-directions?
- Is the intent to account for the fact that a design-basis earthquake may not produce equal earthquake demand (i.e., spectral acceleration) in both the x- and y-directions of a building?
- Is the intent to account for both of the above phenomenon?

It is the opinion of the authors that a 100%+30% criterion, as implemented in ASCE/SEI 7-10 (ASCE, 2010) was explicitly intended to account for correlation between the two directions of ground motion. This is supported by "triggers" in the ASCE/SEI 7-10 direction of loading provisions which necessitate the use of a 100%+30% criterion. For example, a column which forms part of two or more intersecting frames will see axial load from both x- and y-direction ground motions. If the ground motions were perfectly uncorrelated (e.g., for every point in time, the x-direction ground motion was zero whenever the y-direction ground motion existed and vice versa), the axial demand on such a column could be predicted by the larger of the x-direction and y-direction demand taken independently. On the other hand, if the ground motions were even somewhat correlated, the axial demand at each point in time would be a combination of the full x-direction and full y-direction demand.

The direction of loading commentary in ASCE/SEI 7-10 (ASCE, 2010) does not associate a 100%+30% criterion to the fact that design-basis earthquakes may not produce equal earthquake demand in both directions. However, this is not to say that when the code developers introduced the 100%+30% provision they did not intend for it to cover such cases. They may have. But the ASCE/SEI 7-10 direction of loading provisions and corresponding commentary do not seem to support that interpretation.

Research Objectives

The first objective of this research is to evaluate the ability of a 100%+30% criterion to conservatively bound the actual response of instrumented buildings. This is approached in two different ways by asking the following questions:

1. Does 30% of the maximum y-direction response adequately bound the y-direction response at the point in time when the maximum x-direction response occurs (and vice versa)?
2. Does an approximation of the actual response, using a 100%+30% criterion, adequately bound the actual response for every point in time?

The second objective of this research is to determine a more appropriate 100%+XX% criterion, where XX can take on values from 0 to 100, assuming that a 100%+30% criterion is not conservative. This is also approached in two different ways by asking the following sets of questions:

1. For 50% of the data, what XX% of the maximum y-direction response bounds the y-direction response at the point in time when the maximum x-direction response occurs (and vice versa)? What about for 84% of the data?
2. For 50% of the data, what XX% must be used such that an approximation of the actual response, using a 100%+XX% criterion, bounds the actual response for every point in time? What about for 84% of the data?

The third objective of this research is to assess the dependence of these evaluation methods on different building, earthquake and sensor characteristics (e.g., ground motion intensity, ratio of fundamental period in each direction, etc.). Since the results of these studies do

not demonstrate any significant dependence, they have not been included in this paper. The fourth objective is to assess the dependency on using a set of axes rotated to align with the maximum response rather than aligned with the building's axes. The fifth objective is to assess the dependency on the way in which the approximation of the actual response using a 100%+XX% criterion is constructed (see Figure 5).

Methodology

Response Types and Sensor Combinations

The CESMD (2015) records, whether recorded directly by individual sensors (i.e., absolute acceleration) or calculated based on the recorded data (i.e., relative displacement), were used to define three response types.

1. Sensor-to-sensor drift ratio is computed by taking the displacement of a sensor at a chosen floor and subtracting the displacement of a corresponding sensor at the next instrumented floor below at each instant of time. The resulting displacement difference, also known as drift, is then divided by the difference in height between the sensors to produce a dimensionless drift ratio. Figure 1a shows how sensor-to-sensor drift ratio is computed for an example station with the slope of the red line indicating Sensor 11 to Sensor 10 drift ratio.
2. Sensor-to-ground drift ratio is computed by taking the displacement of a sensor at a chosen floor and subtracting the displacement of a corresponding sensor at the base of the building at each instant of time. The resulting displacement difference, also known as drift, is then divided by the difference in height between the sensors to produce a drift ratio. See Figure 1b for an example.
3. Absolute acceleration (the response recorded by the accelerometers) is taken as the acceleration of a sensor at a chosen floor at each instant of time. See Figure 1c for an example.

The evaluation of a 100%+XX% criterion necessarily requires consideration of response in two orthogonal directions. As such, some relation must be established between sensors which measure response in one direction and those which measure response in the perpendicular direction. In the stations from the CESMD (2015), a station north is established based on the axis of the building that most closely aligns with true north. From that, sensors are typically oriented station north-south and station east-west. The task is therefore to define relationships between north-south sensors and corresponding east-west sensors. This creates a pair of sensors at an individual floor which must also be, depending on the response type used, related to a corresponding pair of sensors at another floor. Figure 1 illustrates this process where red and blue sensors measure east-west and north-south response, respectively. A sensor combination for a given station and earthquake is referred to as a station-earthquake-sensor combination in this research. Note that the different response types (i.e., sensor-to-sensor drift ratio, sensor-to-ground drift ratio, and absolute acceleration) require different combinations of sensors. The same sensor combinations for sensor-to-ground drift ratio and absolute acceleration are used in this research so that a displacement-based and acceleration-based response parameter can be

compared for the same station-earthquake-sensor combinations. For further information about sensor combinations, refer to the full report on this research (Zimmerman et al., in preparation).

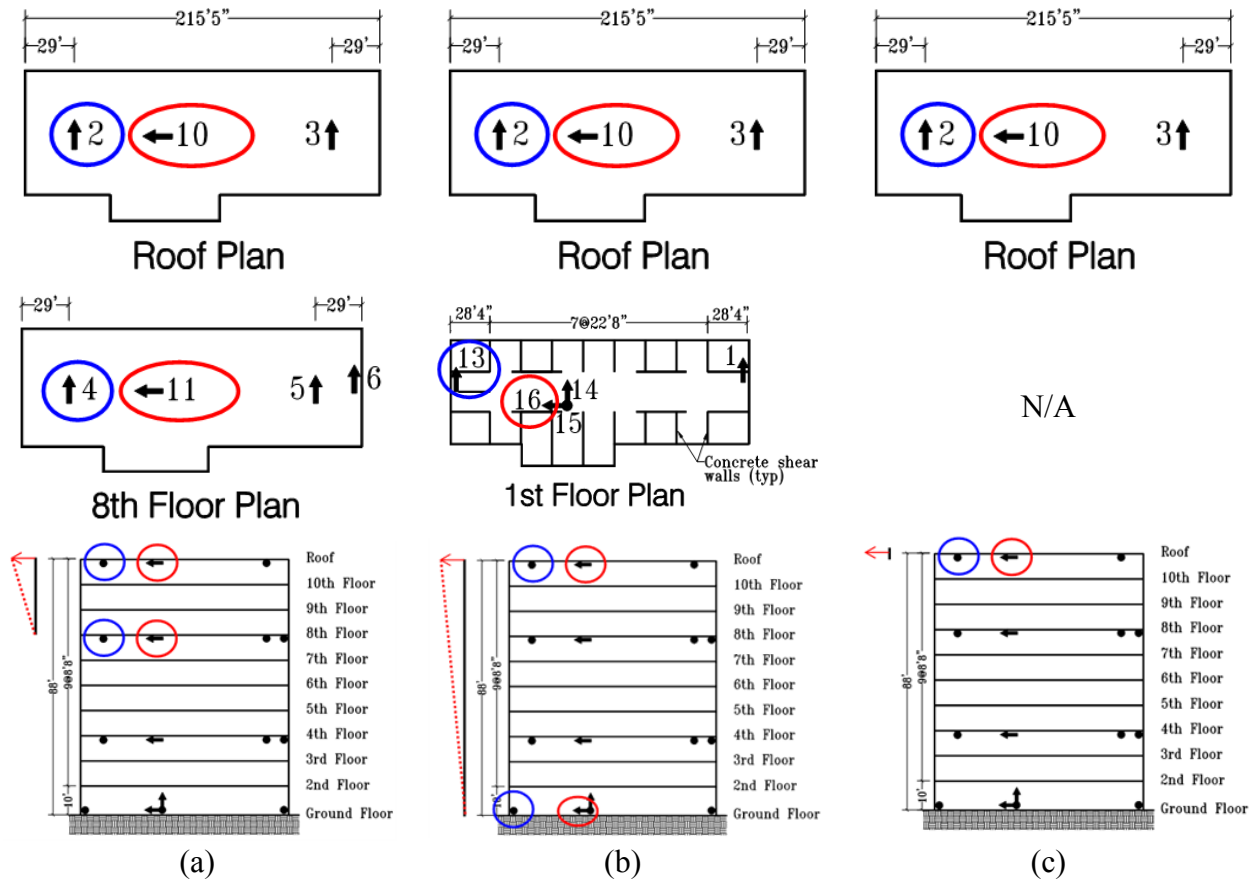


Figure 1. Illustration of (a) sensor-to-sensor drift ratio, (b) sensor-to-ground drift ratio, and (c) absolute acceleration for CSMIP Station No. 24385. Red and blue indicate sensors measuring east-west and north-south, respectively.

CESMD Database

As mentioned previously, this is the first study to use actual building response to assess the direction of loading provisions in ASCE/SEI 7 (ASCE, 2010). The following summarizes the data from CESMD (2015) that was available for this study:

- 182 stations (i.e., buildings) located throughout the State of California
- 144 earthquakes ranging from the Santa Barbara Earthquake in 1978 to the Fontana Earthquake on January 15, 2014
- 860 station-earthquakes, where one station-earthquake represents one earthquake affecting one station. Since each earthquake can affect multiple stations and some stations have records from multiple earthquakes, the number of station-earthquakes exceeds both the number of earthquakes and the number of stations.
- 2,061 station-earthquake-sensor combinations for sensor-to-sensor drift ratio

- 1,787 station-earthquake-sensor combinations for sensor-to-ground drift ratio and absolute acceleration.

In order to arrive at the number of stations, station-earthquakes and station-earthquake-sensor combinations provided above, a comprehensive filtering process was conducted. This process accomplished eliminating unsuitable data, combining the parameters of interest for redundant sensors, and balancing the quality and quantity of the data used. For a complete description, see the full report on this research (Zimmerman et al., in preparation).

Orbital Plots

Orbital plots, such as the one shown in Figure 2, show the response along one direction versus the response along the perpendicular direction.

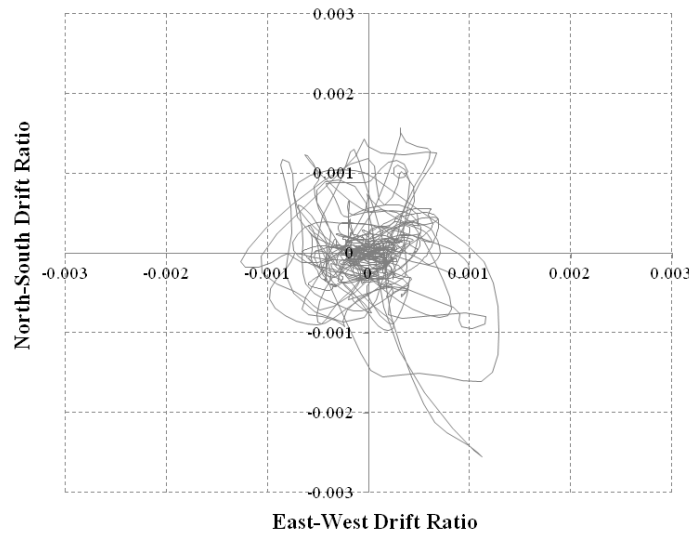


Figure 2. Orbital plot of sensor-to-sensor drift ratio for Station 24385, 1994 Northridge Earthquake, Sensor Combination [11, 4] and [10, 2].

Orthogonal Ratio Study

For the orthogonal ratio study, two points are identified on the orbital plot. The first point corresponds to the maximum east-west response which has coordinates: $(EW_{max}, NS_{atmaxEW})$. The second corresponds to the maximum north-south response which has coordinates: $(EW_{atNSmax}, NS_{max})$. When determining these points, the maximum response is taken as the absolute maximum of both positive and negative values. Therefore, EW_{max} and/or NS_{max} could be a negative number.

Once these two points have been identified, the 100% component or, more specifically, the 100% East-West and the 100% North-South components of a 100%+XX% criterion are known. To determine the percentage contribution in the orthogonal direction, Equations 1 and 2 are used.

$$\alpha_{EW} = \frac{|EW_{atmaxNS}|}{|EW_{max}|} \quad \text{Equation 1}$$

$$\alpha_{NS} = \frac{|NS_{atmaxEW}|}{|NS_{max}|} \quad \text{Equation 2}$$

$$\alpha = \max(\alpha_{EW}, \alpha_{NS}) \quad \text{Equation 3}$$

Equations 1 through 3 are applied for each station-earthquake-sensor combination. Figure 3 shows an example calculation of α_{EW} . Figure 4 shows an example calculation for α_{NS} .

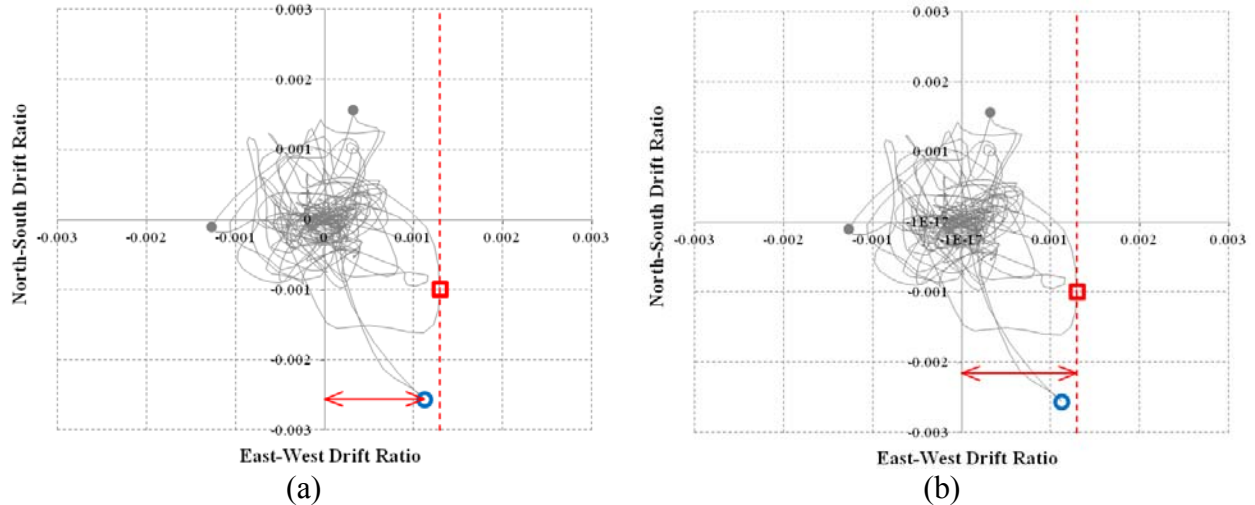


Figure 3. Calculation of $\alpha_{EW} = 87\%$ as the ratio of (a) $|EW_{atmaxNS}| = 0.0011$ to (b) $|EW_{max}| = 0.0013$ for sensor-to-sensor drift ratio for Station 24385, 1994 Northridge Earthquake, Sensor Combination [11, 4] and [10, 2].

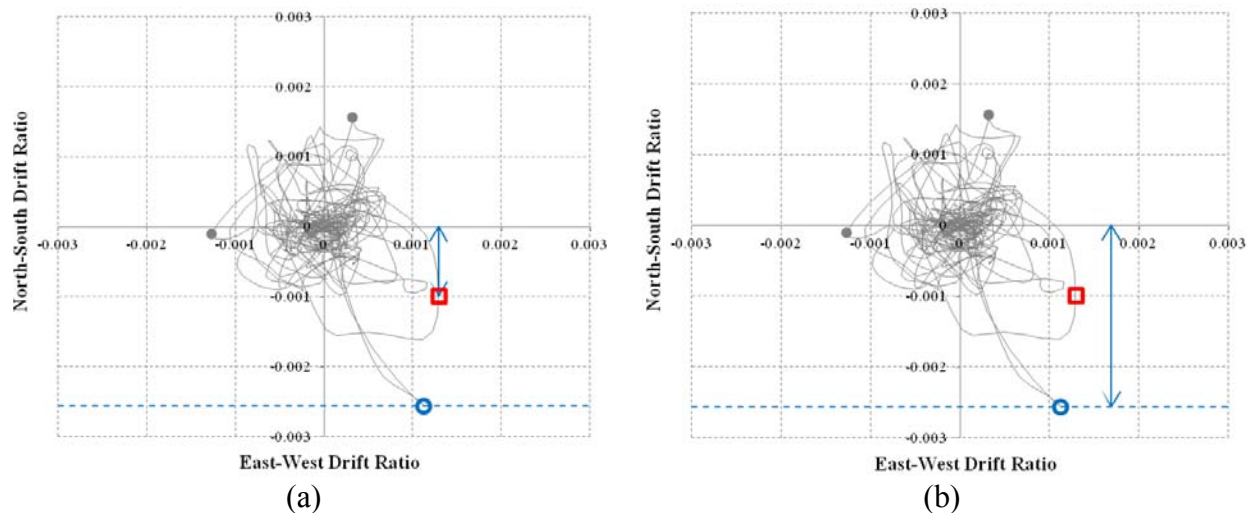


Figure 4. Calculation of $\alpha_{NS} = 39\%$ as the ratio of (a) $|NS_{atmaxEW}| = 0.00098$ to (b) $|NS_{max}| = 0.0026$ for sensor-to-sensor drift ratio for Station 24385, 1994 Northridge Earthquake, Sensor Combination [11, 4] and [10, 2].

Octagon and Truncated Ellipse Interaction Studies

The octagon and truncated ellipse interaction studies approach the evaluation of the 100%+XX% criterion in a slightly different manner than the orthogonal ratio study. They similarly begin by finding EW_{max} and NS_{max} as described for the orthogonal ratio study. However, instead of extracting the orthogonal component of response at these two points, they construct eight control points connected by an interaction interpolation. The eight control points have coordinates in the orbital space as presented in generalized form in Figure 5. For generality, each axis in Figure 5 has been normalized by the maximum response along that axis (i.e., $|EW_{max}|$ or $|NS_{max}|$). Figure 5 also shows three potential interpolations between the control points. Figure 5b and Figure 5c are called octagon interaction and truncated ellipse interaction, respectively, in this research. The justification for the various possible interaction interpolations shown in Figure 5 along with discussion on the relationship between the ASCE/SEI 7-10 requirements and the control nodes can be found in Zimmerman et al. (2014).

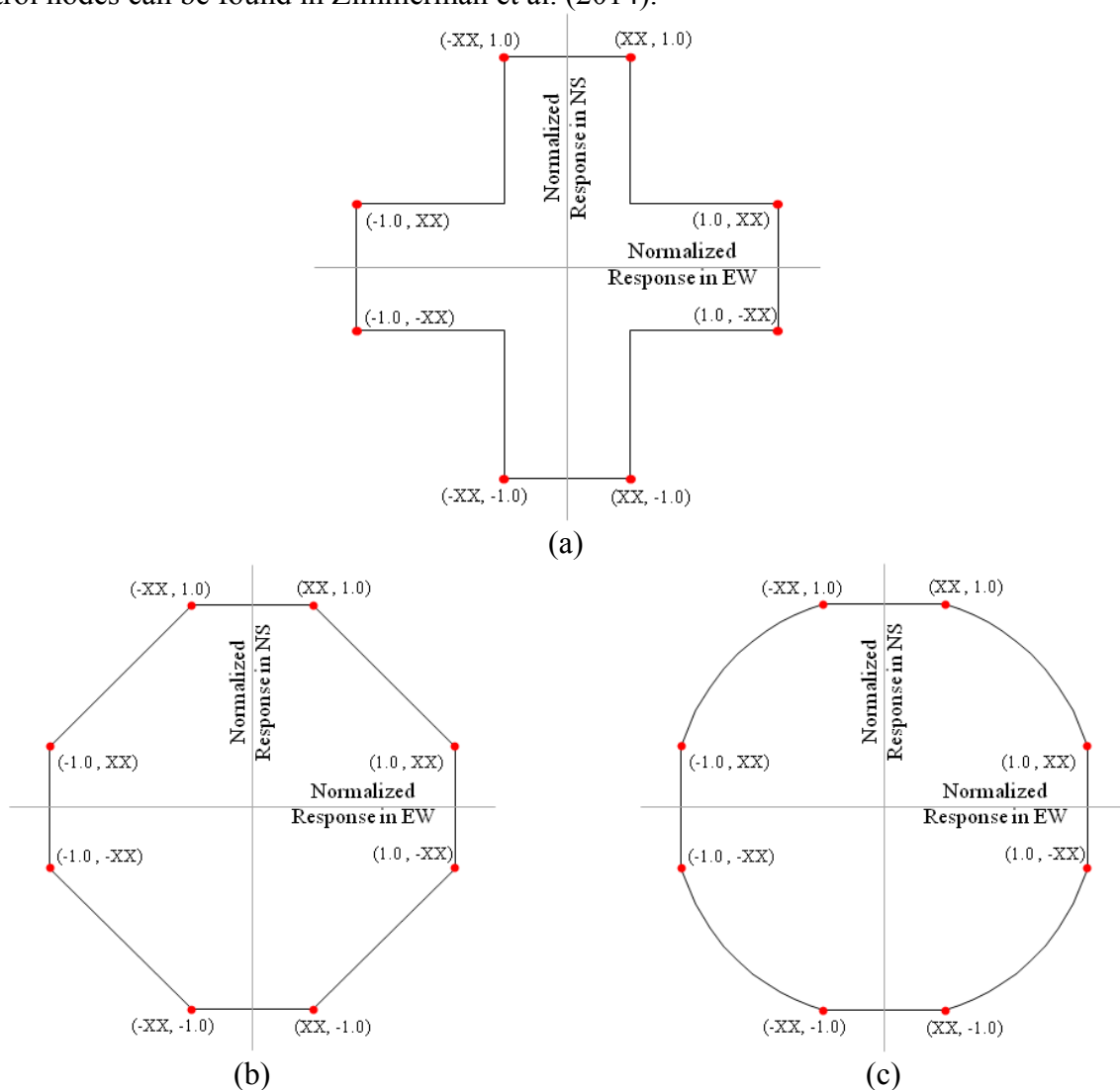


Figure 5. Generalized coordinates of control points for a 100%+XX% criterion and (a) no interpolation on the diagonal, (b) linear interpolation on the diagonal, and (c) elliptical interpolation on the diagonal.

The parameter of interest for the octagon interaction and truncated ellipse interaction studies is termed the response-limit ratio. The response-limit ratio is analogous to the demand-capacity ratio used in structural engineering practice. As the name implies, it is a measure of the ratio of the response to a defined limit. That limit is taken as the octagon interaction or truncated ellipse interaction interpolation. To define the response-limit ratio, two vectors are created for every point in the response history.

The first vector connects the origin of the orbital plot with any point on the response orbital. It represents the radial component of the response. The second vector connects the origin of the orbital plot to a point at the intersection of the interaction interpolation and a line having the same orientation as the first vector (i.e. parallel and in the same quadrant). It is intended to be a quantitative measure of the limit. The response-limit ratio, RLR , is then calculated as the ratio of the length of the response vector to the length of the limit vector. An example of these two vectors can be seen in Figures 6 and 7 for the octagon interaction and truncated ellipse interaction studies, respectively. Note that the RLR can take on values greater than, less than, or equal to 1.0.

The search for the maximum RLR , RLR_{max} , is restricted to the regions of the orbital plot shown on normalized axes in Figure 8. This permits RLR_{max} to take on values greater than, less than, or equal to 1.0.

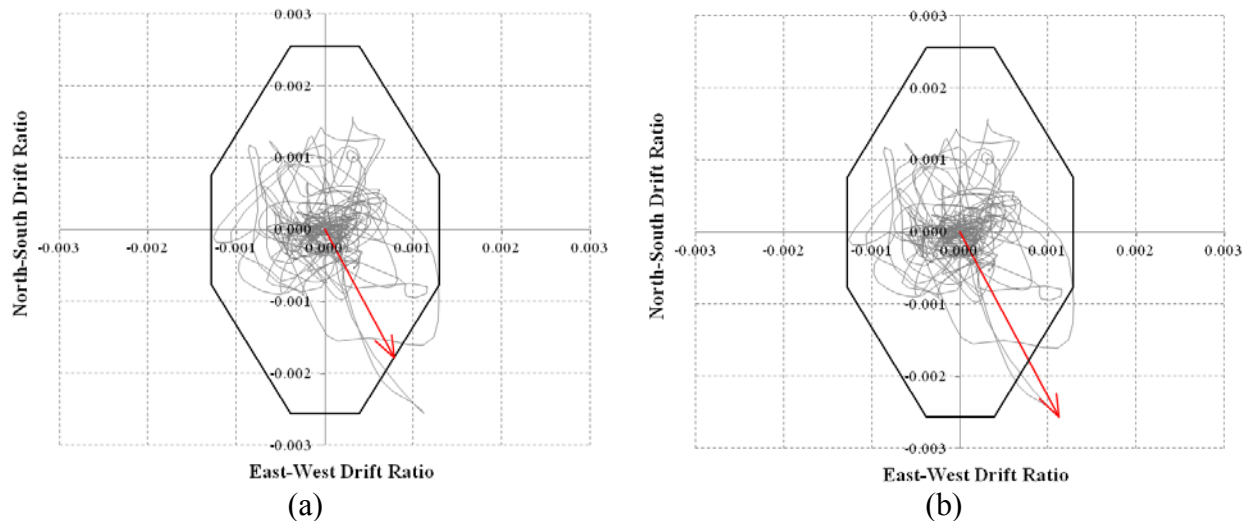


Figure 6. Vectors used to calculate RLR for octagon interaction study where (a) is vector representing response = 0.0019 and (b) is vector representing limit = 0.0028. Vectors shown for point at which $RLR_{max} = 1.44$ occurs in the response history of sensor-to-sensor drift ratio for Station 24385, 1994 Northridge Earthquake, Sensor Combination [11, 4] and [10, 2], and $XX = 0.3$.

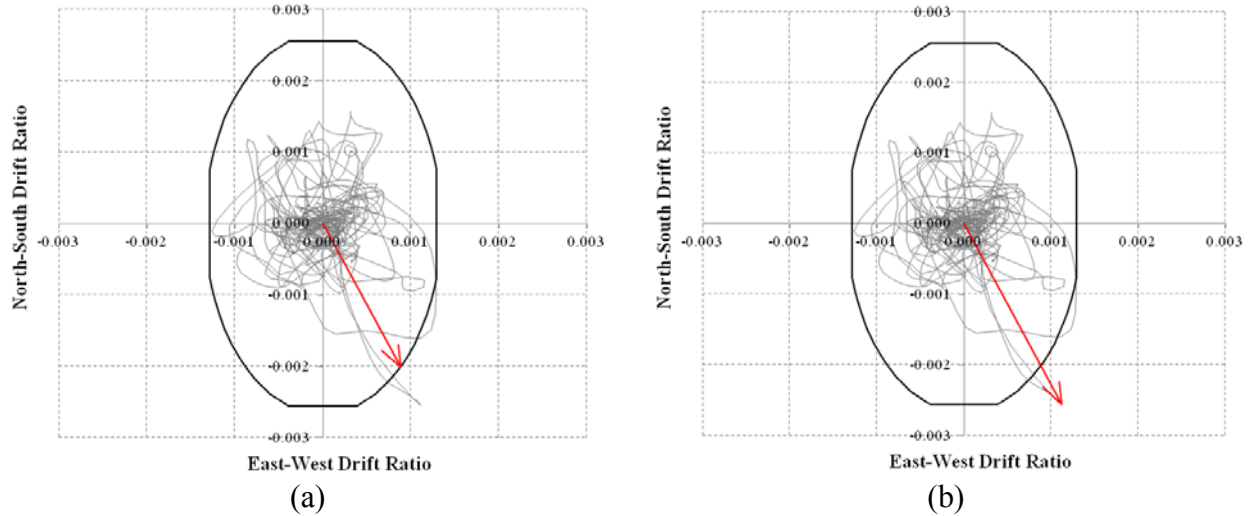


Figure 7. Vectors used to calculate RLR for truncated ellipse interaction study where (a) is vector representing response = 0.0022 and (b) is vector representing limit = 0.0028. Vectors are shown for point at which $RLR_{max} = 1.27$ occurs in the response history of sensor-to-sensor drift ratio for Station 24385, 1994 Northridge Earthquake, Sensor Combination [11, 4] and [10, 2], and $XX = 0.3$.

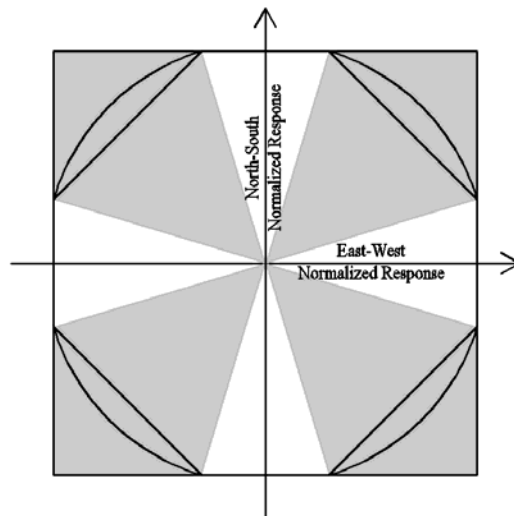


Figure 8. Areas of orbital space in which search for RLR_{max} is restricted shown in grey.

Zone Study

The zone study classifies the response of a specified station-earthquake-sensor combination into one of four "zones" in the orbital space as shown in Figure 9.

Zone 1 corresponds to the region of the orbital space depicted in Figure 5a and represents response which has been directly accounted for by a 100%+XX% criterion. It appears as a cross sign in the orbital space. Station-earthquake-sensor combinations for which all response is within Zone 1 for a given 100%+XX% criterion would be considered to satisfy that criteria explicitly.

Zone 2 corresponds to the region within the octagon interaction interpolation but excluding that already classified as Zone 1. It appears as four triangles, one in each quadrant of the orbital space. Station-earthquake-sensor combinations for which all response is within Zone 1 or Zone 2 for a given 100%+XX% criterion would be considered to satisfy that rule implicitly (under the assumption that linear interpolation between the control points of Figure 5b is appropriate).

Zone 3 corresponds to the region within the truncated ellipse interaction interpolation but excluding that already classified as Zone 1 or Zone 2. It appears as four segments of an ellipse, one in each quadrant of the orbital space. Station-earthquake-sensor combinations for which all response is within Zone 1, 2 or 3 for a given 100%+XX% criterion would be considered to satisfy that rule implicitly (under the assumption that elliptical interpolation between the control points of Figure 5c is appropriate).

Finally, Zone 4 is the region outside of the elliptical interaction interpolation. Station-earthquake-sensor combinations for which any point in the response history is within Zone 4 would be considered to violate that criterion regardless of whether octagon interaction or truncated ellipse interaction is assumed. In this research, the parameter of interest, Z_{crit} , for a given station-earthquake-sensor combination is assigned the value of the highest zone of any point on the response orbital.

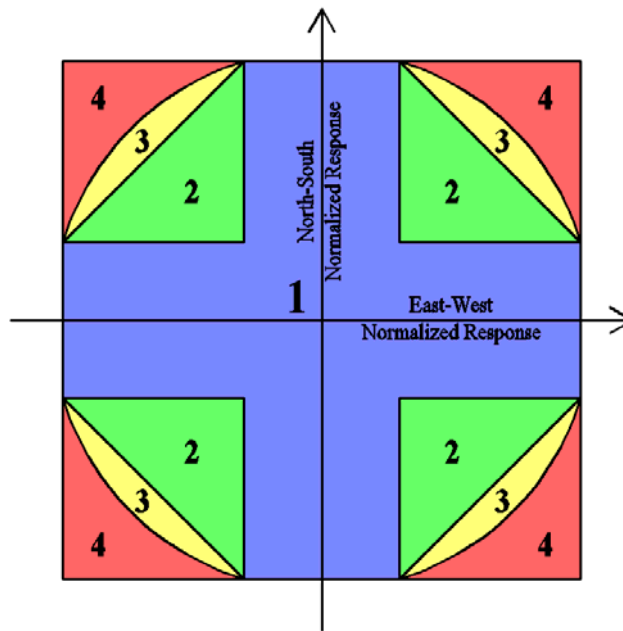


Figure 9. Zones of the orbital space. Zone 1, 2, 3 and 4 shown in blue, green, yellow and red, respectively.

Maximum Direction Study

ASCE/SEI 7-10 (ASCE, 2010), in contrast with its predecessor (ASCE/SEI 7-05), uses the maximum component of ground motion as the basis of design. In this research, the recorded response of the building is used directly to determine the maximum response and the maximum

response direction. The maximum response direction is taken as the orientation of the largest vector from the origin to any point on the response orbital. For example, see Figure 10b where the orientation of maximum response is controlled by the blue circle. After rotating to the maximum direction, all response quantities of interest are recomputed for the maximum direction study. Therefore, the maximum direction study is similar to the methodologies explained previously, only performed in a rotated coordinate system.

The original, unrotated interaction studies recognize that most buildings have a set of axes defined based on their geometry. Even though these axes neglect any influence of ground motion, they are used in the unrotated interaction studies for consistency with the state of engineering practice in regards to the direction of loading provisions in ASCE/SEI 7-10 (ASCE, 2010). The maximum direction study instead recognizes that the building response is the product of both the ground motion and the building characteristics. It therefore attempts to capture the intent of ASCE/SEI 7-10 that the 100% component of the 100%+XX% criteria be based on the maximum response direction, although it only achieves this for one of the two directions.

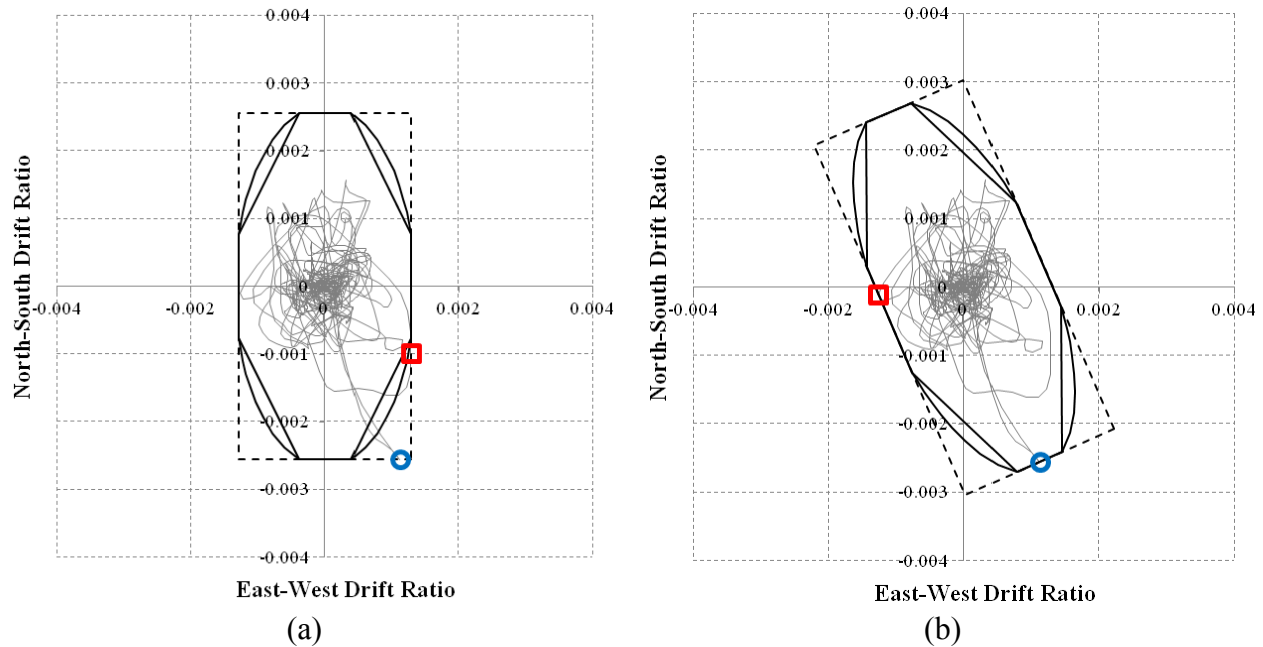


Figure 10. Comparison of (a) unrotated versus (b) rotated-to-maximum direction study. Example shown is for sensor-to-sensor drift ratio for Station 24385, 1994 Northridge Earthquake, Sensor Combination [11, 4] and [10, 2], and $XX = 0.3$.

Equal Interaction Study

The equal interaction study recalculates the response quantities of interest for the original, unrotated octagon interaction and truncated ellipse interaction studies but uses an equal interaction interpolation that has the same dimension in both the East-West and North-South directions. This dimension is taken as the largest of $|EW_{max}|$ and $|NS_{max}|$. For comparison, the octagon interaction and truncated ellipse interaction studies explained earlier used unequal interaction with an East-West dimension based on $|EW_{max}|$ and a North-South dimension based on $|NS_{max}|$. Once the new, equal interaction is constructed, the response quantities of interest are

computed similarly to that described previously. See Figure 11 for a comparison of equal versus unequal interaction.

The equal interaction study is pursued in addition to the unequal interaction study because both ASCE/SEI 7-10 (ASCE, 2010) and the derivation in Rosenblueth and Contreras (1977) assume equal earthquake response spectra in both directions. As noted previously, the recorded building response does not necessarily result from equal earthquake demand in both directions for every station-earthquake-sensor combination. Therefore, the construction of an equal interaction interpolation may not be suitable when considering response from unequal earthquake demand. Additionally, it may not be suitable to construct an equal interaction interpolation when a building is composed of different lateral force-resisting systems in each direction (e.g., moment frame in the x-direction and braced frame in the y-direction) because the response in each direction will be different even if the earthquake demands were equal.

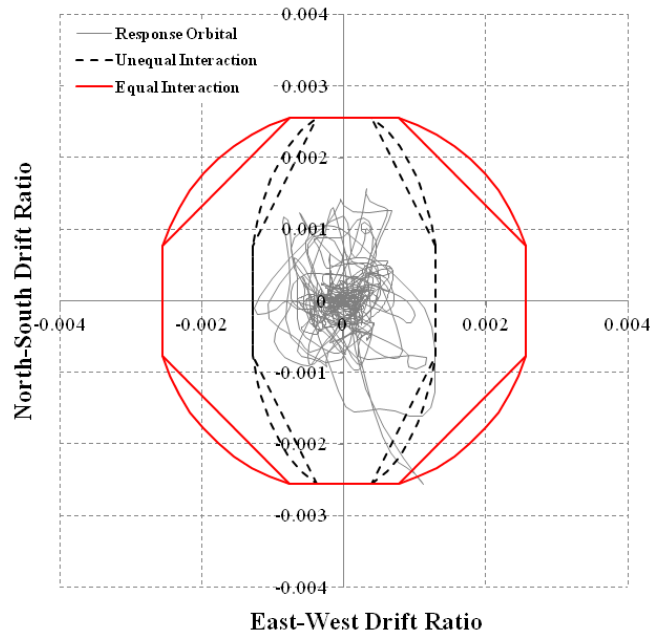


Figure 11. Comparison of unequal versus equal interaction for sensor-to-sensor drift ratio for Station 24385, 1994 Northridge Earthquake, Sensor Combination [11, 4] and [10, 2], and $XX = 0.3$.

Evaluation Methods

There are several evaluation methods pursued in this research. The evaluation methods operate on the parameters of interest (i.e., α , RLR_{max} and Z_{crit}) after assembling the parameters of interest for all station-earthquake-sensor combinations.

The evaluation method applicable for the orthogonal ratio study is the probability of non-exceedance, computed in accordance with Equation 4. The parameter α is calculated using Equation 3 for each station-earthquake-sensor combination and XX is the component of the selected 100%+ XX % criterion. The probability of non-exceedance is therefore equivalent to the probability that α will be less than a selected XX for any given station-earthquake-sensor

combination. By performing the calculation in Equation 4 for each value of XX ranging from 0 to 1.0, a probability of non-exceedance curve can be constructed. See Figure 12 for an example curve of the entire database for sensor-to-sensor drift ratio.

Probability of Non – Exceedance =

$$P(\alpha \leq XX) = \frac{\# \text{ of "station – earthquake – sensor combinations" for which } \alpha \leq XX}{\text{total \# of "station – earthquake – sensor combinations"}}$$

Equation 4

The probability of non-exceedance is also an evaluation method used for the octagon interaction and truncated ellipse interaction studies. In this case, however, the probability of non-exceedance is computed via Equation 5. $RLLR_{max}$ is the maximum response limit ratio for each station-earthquake-sensor combination with the limit taken in accordance with the octagon interaction or truncated ellipse interaction interpolations for a chosen 100%+XX% criterion. $RLLR_{max}$ equals 1.0 when the response and limit are equal. The probability of non-exceedance is therefore equivalent to the probability that $RLLR_{max}$ will be less than or equal to 1.0 for any given station-earthquake-sensor combination. By performing the calculation in Equation 5 for each value of XX ranging from 0 to 1.0, a probability of non-exceedance curve can be constructed. See Figure 13 for example curves of the entire database for sensor-to-sensor drift ratio.

Probability of Non – Exceedance =

$$P(RLLR_{max} \leq 1.0) = \frac{\# \text{ of "station – earthquake – sensor combinations" for which } RLLR_{max} \leq 1.0}{\text{total \# of "station – earthquake – sensor combinations"}}$$

Equation 5

The probability that Z_{crit} for a given station-earthquake-sensor combination will be less than or equal to each of the four zones defined in Figure 9 is another evaluation method. It is computed via Equation 6. Z_{crit} is the value of the highest zone for any point on the response orbital for a given station-earthquake-sensor combination and 100%+XX% criterion. By performing the calculation in Equation 6 for each value of XX ranging from 0 to 1.0, a probability curve can be constructed. See Figures 14 through 16 for example curves of the entire database for sensor-to-sensor drift ratio. Note that the probability for this evaluation method is expressed as the probability that Z_{crit} is less than or equal to the selected zone (i.e., not that Z_{crit} is equal to the selected zone). To calculate the probability that Z_{crit} is equal to the selected zone, Equation 7 can be used. For example, the probability that Z_{crit} is equal to Zone 3 would be the probability that Z_{crit} is less than or equal to Zone 3 minus the probability that Z_{crit} is less than or equal to Zone 2.

$$P(Z_{crit} \leq \text{zone}) = \frac{\# \text{ of "station – earthquake – sensor combinations" for which } Z_{crit} \leq \text{zone}}{\text{total \# of "station – earthquake – sensor combinations"}}$$

Equation 6

$$P(Z_{crit} = \text{zone}) = P(Z_{crit} \leq \text{zone}) - P(Z_{crit} \leq \text{zone} - 1)$$

Equation 7

Results

Orthogonal Ratio, Octagon Interaction and Truncated Ellipse Interaction Studies

Figure 12 presents the probability of non-exceedance curve for the orthogonal ratio study using sensor-to-sensor drift ratios. Similar figures exist for sensor-to-ground drift ratio and absolute acceleration but are excluded here for brevity. Several arrows are drawn that intersect the probability of non-exceedance curve. These identify (1) the probability of non-exceedance given a 100%+30% criterion, (2) the 100%+XX% criterion corresponding to a probability of non-exceedance of 50%, and (3) the 100%+XX% criterion corresponding to a probability of non-exceedance of 84%. Probabilities of non-exceedance of 50% and 84% were selected because they represent the mean and mean plus one standard deviation of a normally distributed random variable. The use of these probabilities does not imply that the underlying data fits a normal distribution, however.

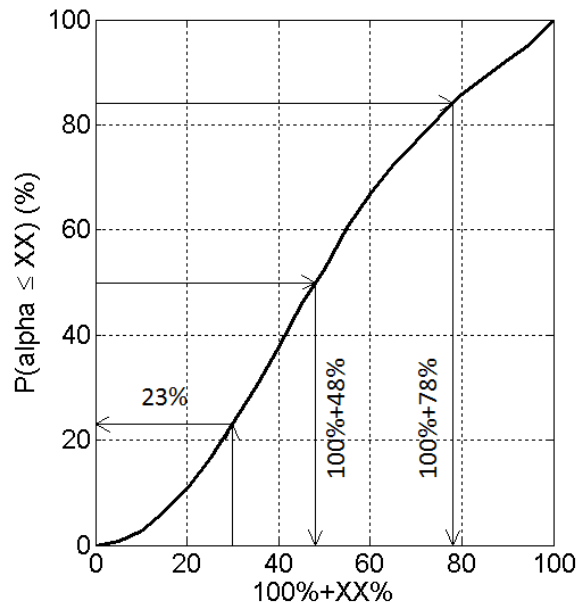


Figure 12. Probability of non-exceedance curve of the orthogonal ratio study using the entire database of sensor-to-sensor drift ratios.

Figure 13a and Figure 13b present the probability of non-exceedance curves for the octagon and truncated ellipse interaction studies, respectively, using sensor-to-sensor drift ratio. Similar figures exist for sensor-to-ground drift ratio and absolute acceleration but are excluded here for brevity. Similar to the results of the orthogonal ratio study, several arrows which intersect the probability of non-exceedance curves at critical points are drawn.

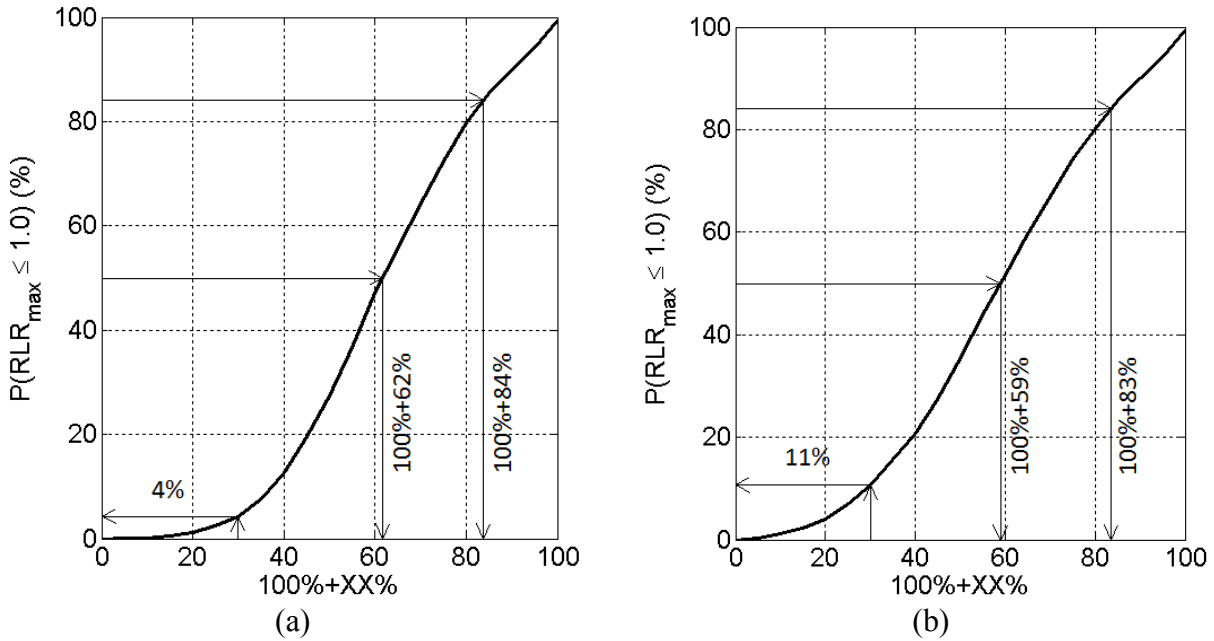


Figure 13. Probability of non-exceedance curves for the (a) octagon and (b) truncated ellipse interaction studies using the entire database of sensor-to-sensor drift ratios.

Tables 1 through 4 present the three critical points described above which intersect the probability of non-exceedance curves and include sensor-to-ground drift ratio and absolute acceleration as well as sensor-to-sensor drift ratio. The results from all response types are fairly consistent both in magnitude (e.g., the 50% probability of non-exceedance corresponds to approximately a 100%+60% criterion for all response types for the octagon interaction study) and in trend (e.g., for all response types, the orthogonal ratio study generally produces the highest probability of non-exceedance followed by the truncated ellipse interaction study and lastly by the octagon interaction study). Furthermore, they all show very low probabilities of non-exceedance (i.e., the data is not adequately bounded) for a 100%+30% criterion.

Table 1. 100%+XX% criterion necessary to satisfy given probabilities of non-exceedance for sensor-to-sensor drift ratio

Probability of Non-Exceedance	Orthogonal Ratio Study	Octagon Study	Truncated Ellipse Study
50%	100%+48%	100%+62%	100%+59%
84%	100%+78%	100%+84%	100%+83%

Table 2. 100%+XX% criterion necessary to satisfy given probabilities of non-exceedance for sensor-to-ground drift ratio

Probability of Non-Exceedance	Orthogonal Ratio Study	Octagon Study	Truncated Ellipse Study
50%	100%+47%	100%+62%	100%+59%
84%	100%+78%	100%+83%	100%+83%

Table 3. 100%+XX% criterion necessary to satisfy given probabilities of non-exceedance for absolute accelerations

Probability of Non-Exceedance	Orthogonal Ratio Study	Octagon Study	Truncated Ellipse Study
50%	100%+44%	100%+58%	100%+55%
84%	100%+71%	100%+78%	100%+78%

Table 4. Probability of non-exceedance given selection of a 100%+30% criterion

Response Parameter	Orthogonal Ratio Study	Octagon Study	Truncated Ellipse Study
Sensor-to-Sensor Drift Ratio	23%	4%	11%
Sensor-to-Ground Drift Ratio	23%	4%	11%
Absolute Acceleration	27%	5%	13%

Zone Study

Figures 14 through 16 present the probability that Z_{crit} will be less than or equal to a selected zone for sensor-to-sensor drift ratio. Similar figures exist for sensor-to-ground drift ratio and absolute acceleration but are excluded here for brevity. Note that Figures 14 through 16 are identical except for the arrows which intersect the probability curves. Similar to the previous studies, these arrows identify (1) the probability given a 100%+30% criterion, (2) the 100%+XX% criterion corresponding to a probability of 50%, and (3) the 100%+XX% criterion corresponding to a probability of 84%.

Probability values shown in Figure 14 are for the probability that Z_{crit} will be less than or equal to a selected zone. Equation 7 must be used if the probability that Z_{crit} is equal to a selected zone is desired. For example, in Figure 14, the probability that Z_{crit} is equal to Zone 4 is $100\% - 9\% = 91\%$ while the probability that Z_{crit} is equal to Zone 3 is $9\% - 4\% = 5\%$. In Figures 15 and 16, a 100%+XX% criterion corresponding to a given probability is shown. For example, a 100%+63% criterion bounds 50% of the data in Zones 1, 2 or 3 while a 100%+77% criterion would be required to bound 50% of the data in Zone 1 only. The probability curve separating Zone 3 from Zone 4 approximately matches the probability of non-exceedance curve for the truncated ellipse interaction study while the curve separating Zone 2 from Zone 3 approximately matches that for the octagon interaction study. Refer to full report on this research for further explanation on the similarity between the probability curves in the zone study as compared to the octagon and interaction studies (Zimmerman et al., in preparation).

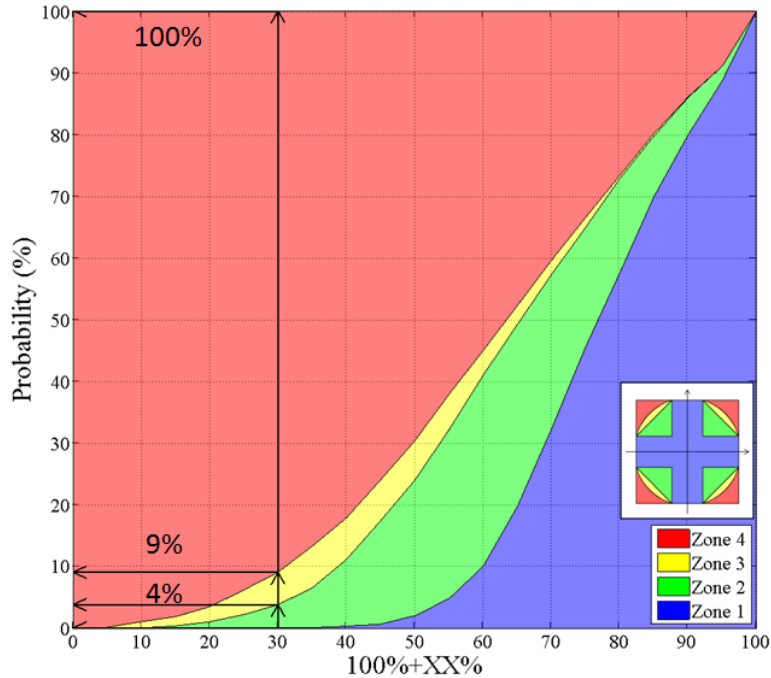


Figure 14. Probability that Z_{crit} for a given station-earthquake-sensor combination will be less than or equal to each of the zones for the entire database of sensor-to-sensor drift ratios. Probabilities specifically indicated are for a 100%+30% criterion. The probability that Z_{crit} is in Zone 1 is too small to show and has therefore been left off the figure.

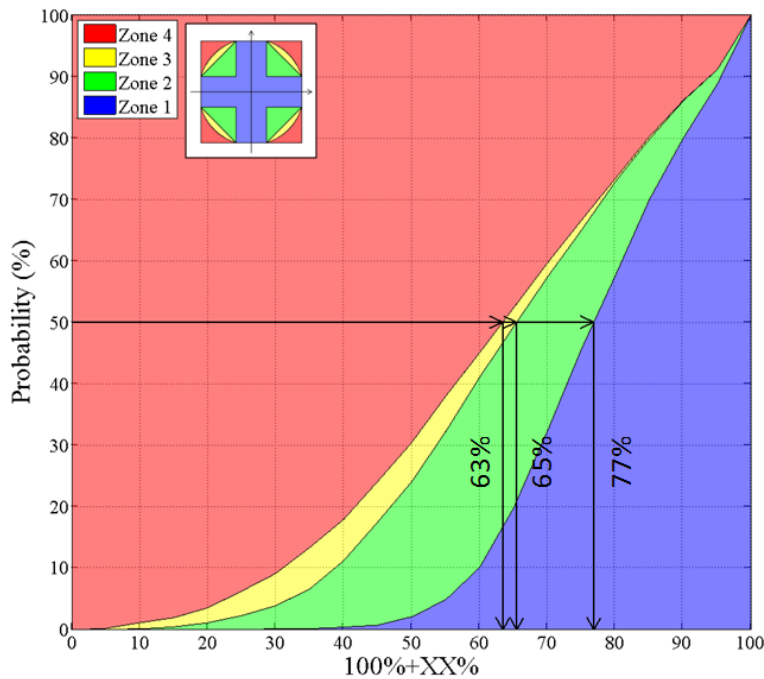


Figure 15. Probability that Z_{crit} for a given station-earthquake-sensor combination will be less than or equal to each of the zones for the entire database of sensor-to-sensor drift ratios. The 100%+XX% criteria necessary to bound 50% of the data is indicated.

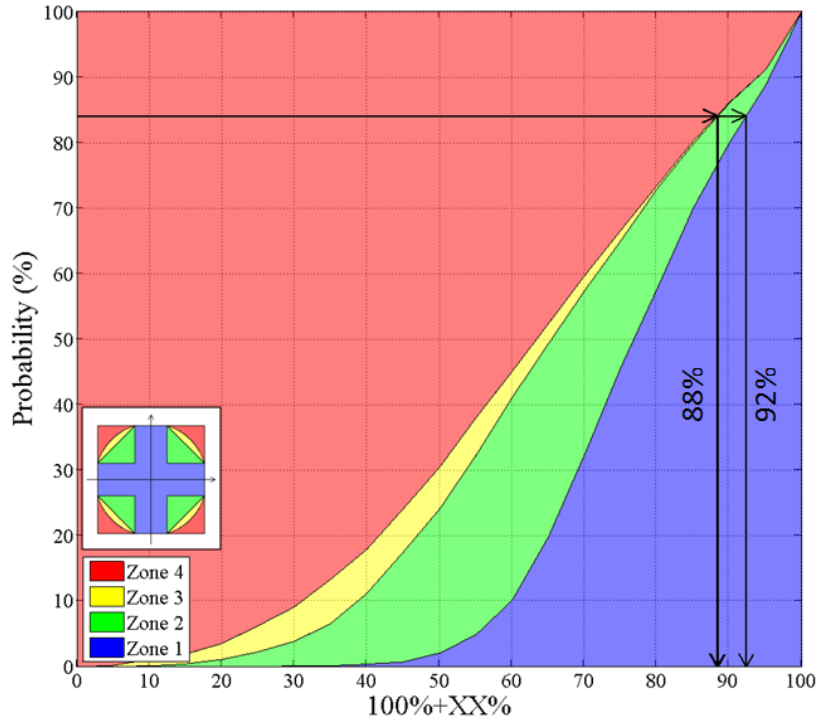


Figure 16. Probability that Z_{crit} for a given station-earthquake-sensor combination will be less than or equal to each of the zones for the entire database of sensor-to-sensor drift ratios. The 100%+XX% criteria necessary to bound 84% of the data is indicated.

Maximum Direction Study

Figure 17 and Figure 18 present the probability of non-exceedance curves for the orthogonal ratio and interaction studies, respectively, considering both unrotated and rotated-to-maximum-direction methodologies using sensor-to-sensor drift ratios. Similar figures exist for sensor-to-ground drift ratio and absolute acceleration but are excluded here for brevity. The unrotated probability of non-exceedance curves are identical to those shown in Figures 12 and 13. The probabilities of non-exceedance for the maximum direction study are significantly greater than those for the unrotated studies. This indicates that when the studies are performed in a coordinate system rotated to align with the maximum direction of response, more of the data are bounded for a given 100%+XX% criterion.

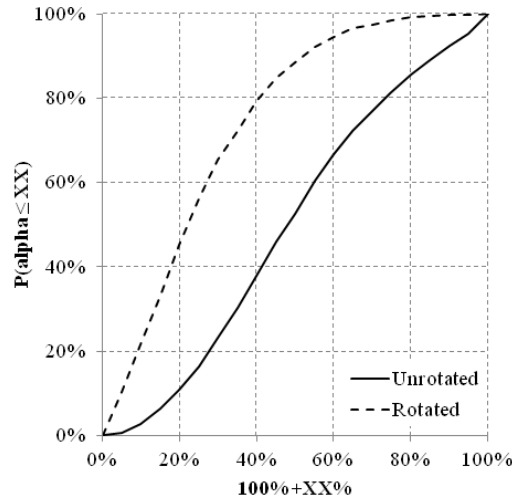


Figure 17. Comparison of unrotated versus rotated-to-maximum-direction probability of non-exceedance curves for the orthogonal ratio study using sensor-to-sensor drift ratio.

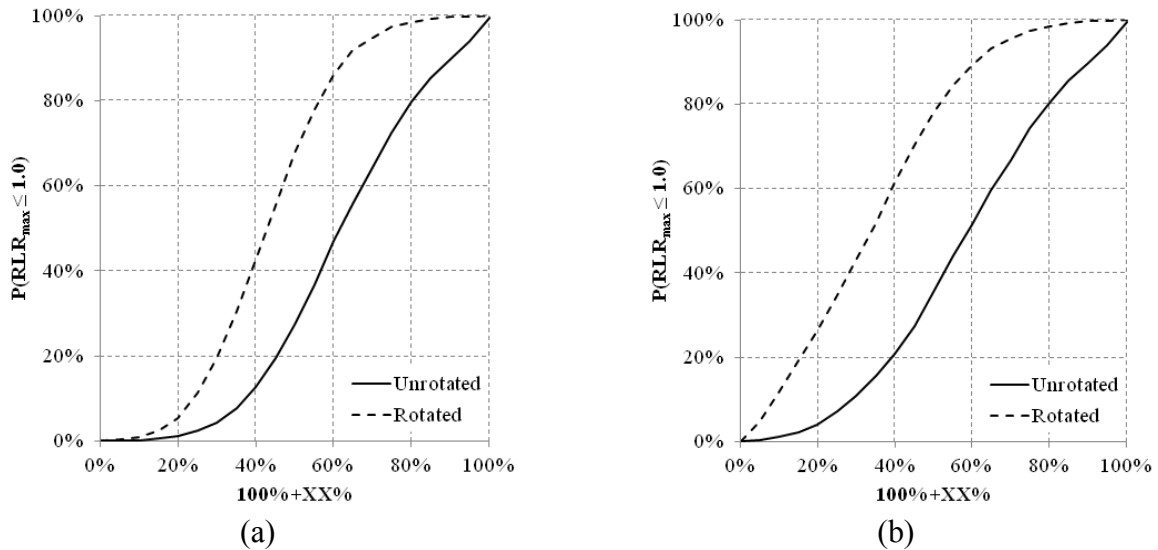


Figure 18. Comparison of un-rotated versus rotated-to-maximum-direction probability of non-exceedance curves for the (a) octagon interaction and (b) truncated ellipse interaction studies using sensor-to-sensor drift ratio.

Equal Interaction Study

Figure 19 presents the probability of non-exceedance curves considering both the original, unequal interaction and equal interaction interpolations. Similar figures exist for sensor-to-ground drift ratio and absolute acceleration but are excluded here for brevity. The probability of non-exceedance curves for unequal interaction are identical to those shown in Figure 13. The probabilities of non-exceedance for equal interaction are significantly greater than the results for unequal interaction. This indicates that when the studies are performed using an equal interaction interpolation, more of the data are bounded for a given 100%+XX% criterion.

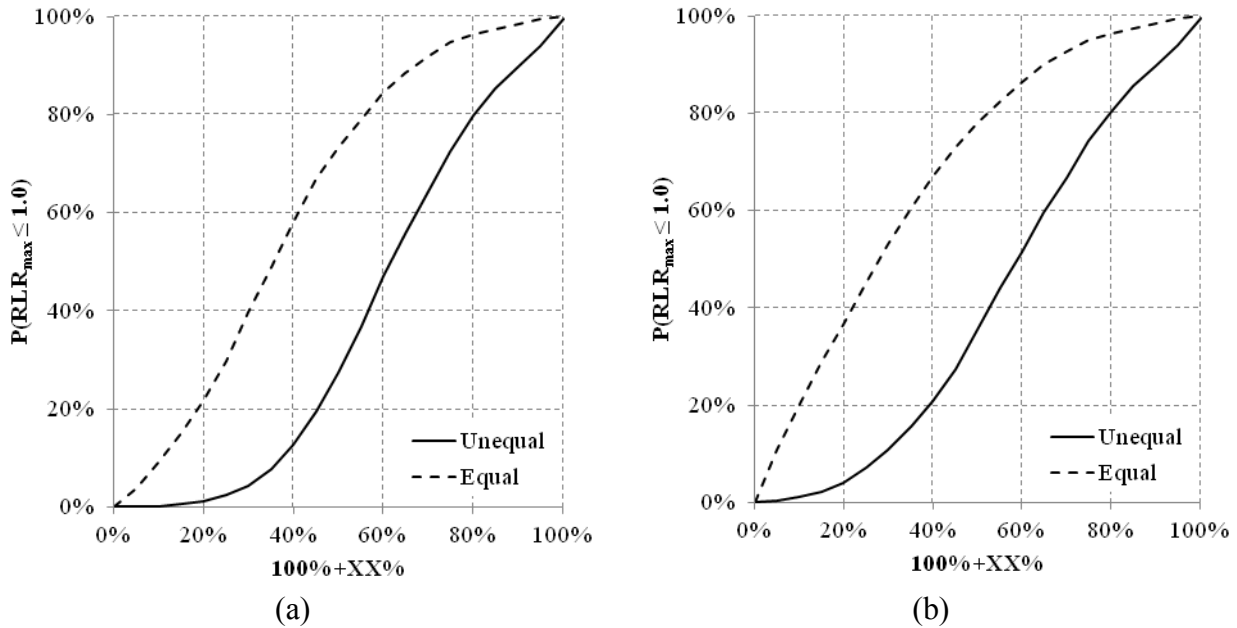


Figure 19. Comparison of probability of non-exceedance curves for equal versus unequal interaction for the (a) octagon interaction and (b) truncated ellipse interaction studies using sensor-to-sensor drift ratio.

Conclusions

Based on results from several evaluation methodologies, response types and a sufficiently populated database obtained from the Center for Engineering Strong Motion Data (CESMD, 2015), the following conclusions are made:

- The 100%+30% criterion, as applied to the response of instrumented buildings during real earthquakes, does not adequately bound the recorded data using all three evaluation methodologies considered in this research (i.e., orthogonal ratio, octagon interaction and truncated ellipse interaction) assuming an unrotated, unequal interaction. To bound 50% and 84% of the data, 100%+60% and 100%+80% criteria, respectively, would be needed.
- The 100%+XX% criterion is fairly insensitive to the three response types used in this research (i.e., sensor-to-sensor drift ratio, sensor-to-ground drift ratio and absolute acceleration).
- Use of the maximum direction of response significantly reduces the estimation of conservatism of the 100%+30% criterion as compared to when the building axes are used. However, it still generally predicts that a 100%+30% criterion does not adequately bound the recorded data. To bound 50% and 84% of the data, 100%+40% and 100%+55% criteria, respectively, would be needed.
- Use of an equal interaction construction significantly reduces the estimation of conservatism of a 100%+30% criterion as compared to the unequal interaction pursued in all other studies. It predicts that the 100%+30% is slightly inadequate in bounding 50% of the recorded data. To bound 50% and 84% of the data, 100%+35% and 100%+60% criteria, respectively, would be needed.

While the conclusions of this research generally find that a 100%+30% criterion does not adequately bound the data, further research is necessary to understand the implications of these findings on the direction of loading provisions in ASCE/SEI 7-10 (ASCE, 2010) and to determine whether revisions are warranted.

Acknowledgements

This paper was developed under research funded by the California Department of Conservation, California Geological Survey, Strong Motion Instrumentation Program, Contract 1012-957. However, the contents do not necessarily represent the policy of that agency nor endorsement by the State Government.

The authors are grateful to Anthony Shakal and Moh Huang of the Strong Motion Instrumentation Program (SMIP) for their assistance and advice during the project, and to the recommendations and comments provided by members of the SMIP Building Subcommittee of the Strong Motion Instrumentation Advisory Committee. Building Subcommittee members included Farzad Naiem, Lucie Fougner, Donald Jephcott, Ifa Kashefi, David Leung, Eduardo Miranda, John Robb, Dan Shapiro, Chris Tokas, and Chia-Ming Uang.

References

- ASCE (2010). *Minimum Design Loads for Buildings and Other Structures, ASCE/SEI 7-10*. American Society of Civil Engineers, Reston, Virginia.
- Bisadi, V., and Head, M., (2011). "Evaluation of Combination Rules for Orthogonal Seismic Demands in Nonlinear Time History Analysis of Bridges," *Journal of Bridge Engineering, Special Issue: AASHTO-LRFD Bridge Design and Guide Specifications: Recent, Ongoing, and Future Refinements*, p711-717.
- "Center for Engineering Strong Motion Data (CESMD)," *strongmotioncenter.org*, Accessed October 14, 2015.
- Cimellaro, G., Giovine, T. and Lopez-Garcia, D. (2014). "Bidirectional Pushover Analysis of Irregular Structures," *Journal of Structural Engineering*, Vol. 140, No. 9, 04014059.
- FEMA (2009). *Quantification of Building Seismic Performance Factors, FEMA P695*. Federal Emergency Management Agency, Washington, D.C.
- Hernandez, J. J. and Lopez, O. A., (2002). "Response to Three-Component Seismic Motion of Arbitrary Direction," *Earthquake Engineering and Structural Dynamics*, Vol. 31, p55-77.
- Lopez, O. A., Chopra, A. K. and Hernandez, J. J., (2001). "Evaluation of Combination Rules for Maximum Response Calculation in Multicomponent Seismic Analysis," *Earthquake Engineering and Structural Dynamics*, Vol. 30, p1379-1398.
- MacRae, G. and Mattheis, J., (2000). "Three-Dimensional Steel Building Response to Near-Fault Motions," *Journal of Structural Engineering*, Vol. 126, Issue 1, p117-126.
- MacRae, G. A. and Tagawa, H., (2001). "Seismic Behavior of 3D Steel Moment Frame with Biaxial Columns," *Journal of Structural Engineering*, Vol. 127, No. 5, p490-497.

- Menun, C. and Der Kiureghian, A., (1998). "A Replacement for the 30%, 40% and SRSS Rules for Multicomponent Seismic Analysis," *Earthquake Spectra*, Vol. 14, No. 1, p153-163.
- Newmark, N.M., (1975). "Seismic Design Criteria for Structures and Facilities - Trans-Alaska Pipeline System," *Proceedings of the U.S. National Conference on Earthquake Engineering*, Ann Arbor, USA, p94-103.
- Rosenblueth, E. and Contreras, H. (1977). "Approximate Design for Multicomponent Earthquakes," *Journal of the Engineering Mechanics Division*, Proceedings of ASCE, Vol. 103, No. EM5, p 881-893.
- Sherman, J. and Okazaki, T., (2010). "Bidirectional Loading Behavior of Buckling-Restrained Braced Frames," *Proceedings of ASCE Structures Congress 2010*, Orlando, Florida.
- Zaghlool, B. S., Carr, A. J. and Moss, P. J., (2001). "Inelastic Behavior of Three-Dimensional Structures under Concurrent Seismic Excitations," *Proceedings of 12th World Conference on Earthquake Engineering*, EQC, Auckland, New Zealand.
- Zimmerman, R. B., Lizundia, B. and Fathali, S., (2014). "Studying Direction of Loading Provisions in Modern Codes: Research Motivation and Literature Review," *Proceedings of the 2014 Strong Motion Instrumentation Program (SMIP14) Seminar*, Berkeley, CA.
- Zimmerman, R.B., Lizundia, B. and Fathali, S., (in preparation). *Evaluation of ASCE/SEI 7 Direction of Loading Provisions Using Strong Ground Motion Records*, Report prepared for the California Strong Motion Instrumentation Program, Data Interpretation Project, Agreement 1012-957.

